Stimulated Growth of Coherent VLF Waves in the Magnetosphere

G. S. STILES[1]

University of California, Los Alamos Scientific Laboratory, Los Alamos, New Mexico 87545

R. A. HELLIWELL

Radioscience Laboratory, Stanford University, Stanford, California 94305

The amplitude behavior of several hundred VLF whistler mode pulse signals and of their associated artificially stimulated emissions (ASE's) has been analyzed with digital signal processing techniques. A survey of the results indicates that the pulse signals characteristically show exponential growth with time that is highly repeatable over short periods. However, the growth rate varies widely from time to time, covering a range of 25–250 dB/s. During the exponential growth phase of the pulse there is no observable change in frequency. Emissions may begin when growth stops or when the input pulse terminates, whichever occurs first. Low growth rates and falling emissions characterize the beginning and ending of extended periods of emission activity. Rising emissions are prominent at the height of activity. ASE's triggered by station NAA (14.7 kHz, 1 MW radiated) begin when the transmitted Morse dash terminates (dash length, 150 ms). Some ASE's triggered by pulses from Siple Station, Antarctica (1.6–7 kHz, ≤1 kW), and Omega, New York (10.2 kHz, 100 W), show similar behavior; others, however, begin prior to the termination of the triggering pulse when the pulse length exceeds 200 ms. Growth and frequency change of the ASE tend to be independent of one another. For transmitted pulses of sufficient duration the amplitude saturates prior to termination. Signal amplitudes may reach 30 dB or more above the initial level. During growth the measured bandwidth of the signal remains near the minimum possible (~27 Hz) with the given analysis resolution (~30 ms, ~50 Hz). By comparison with mathematical models it is shown that the observed signals have the maximum possible coherence for the measured values of growth rate and duration. These observations are in qualitative agreement with a model that attributes signal growth and ASE's to an interaction between coherent waves and counterstreaming gyroresonant electrons.

1. INTRODUCTION

VLF whistler mode waves injected into the magnetosphere from the ground produce a variety of interesting and important effects. For example, whistlers, excited by lightning impulses, are used to map the spatial distribution and drift of plasma within the plasmasphere [*Carpenter and Park*, 1973]. Whistlers and whistler-triggered emissions dump electrons into the ionosphere, exciting bremsstrahlung X rays [*Rosenberg et al.*, 1971] and causing perturbations in electron density that affect subionosphere VLF propagation [*Helliwell et al.*, 1971]. Such perturbations may also excite ULF waves [*Bell*, 1976]. Coherent VLF waves from a controlled ground source grow exponentially with time and trigger a variety of emissions [*Helliwell and Katsufrakis*, 1974]. Radiation from power transmission systems causes similar effects [*Helliwell et al.*, 1975]. Thus whistler mode waves provide a means for both sensing and controlling the properties of the magnetosphere and ionosphere. They may also be of interest for communication and for new types of plasma experiments. It is important therefore to understand the mechanisms that govern the growth of VLF signals and the generation of emissions.

In the present paper we examine the growth aspects of the artificially stimulated VLF emissions (ASE's) given by *Helliwell and Katsufrakis* [1974] and *Stiles and Helliwell* [1975]. The first paper reported measurements of the exponential growth of coherent signals from a VLF transmitter located at Siple Station, Antarctica, and some properties of the associated emissions. The second paper treated the frequency-time characteristics of ASE's from station NAA (14.7 kHz, 1 MW), Omega (10.2 kHz, 100 W), and Siple Station, Antarctica (5.5 kHz, 400 W). For all three sources the triggered emissions, both rising and falling, showed an initial highly repeatable rise in frequency beginning at the triggering frequency. Following the initial rise the ASE either continued to rise, becoming a 'riser,' or reversed its slope, becoming a 'faller.'

To simplify the discussion, we have altered slightly the terminology employed by *Stiles and Helliwell* [1975]. There we included the amplified component of the triggering signal as part of the emission itself. However, it is often difficult to separate the amplified component of the signal from the unamplified component. Accordingly, we shall define an emission as constituting only those components whose frequencies differ measurably from the frequency of the triggering signal or that appear at times when there is no input signal present.

To illustrate the general nature of the phenomena under study, we refer to Figure 5, which shows dynamic spectra of amplified signals and their associated emissions. The many vertical lines on the spectrogram are impulsive signals (sferics) from lightning; they can affect the accuracy of the analysis. The continuous horizontal lines are induced by harmonic currents in the local power system.

In section 2 we describe our method of quantitative spectrum analysis. In section 3 we apply this method to several individual events. Apart from being particularly free of interference from sferics these events are fairly representative of the hundreds that have been examined. Each example will illustrate one or more important features of the growth process. In the final section we summarize and interpret our findings.

2. METHOD OF MEASUREMENT

The major portion of the analysis procedure has been described by *Stiles and Helliwell* [1975]. Broad band VLF analog

[1] Now at Center for Research in Aeronomy, Utah State University, Logan, Utah 84322.

Paper number 6A0732.

recordings are filtered to select the signals of interest; these signals are then digitized. The digital signal is fast-Fourier-transformed [*Bergland*, 1969], and the resulting spectra are stored on digital tape. These spectra may then be averaged as desired to bring out the features of interest.

In the present work we have extended our analysis procedure (summarized by *Stiles* [1974*a*] and described in detail by *Stiles* [1974*b*]) to provide more precise estimates of the frequencies, amplitudes, and bandwidths of the signals under study. These estimates are based upon summations over those components of the spectrum that contain the signal.

The spectrum resulting from the fast Fourier transform of a band-limited wave form $V(t)$ (perhaps containing several signals) may be expressed as [*Otnes and Enochson*, 1972]

$$A_j = \sum_{k=0}^{N-1} V_k e^{-i2\pi jk\Delta f\Delta t} \qquad j = -\frac{N}{2}, \frac{N}{2} \tag{1}$$

where

A_j amplitude of the jth spectral component;
V_k kth sample of the wave form $V(t)$, identical to $V(k\Delta t)$;
Δt spacing in time between the samples of $V(t)$;
Δf spacing in frequency between the components of the spectrum, equal to $1/N\Delta t$;
N total number of samples of $V(t)$.

If $V(t)$ consists of several discrete signals reasonably well spaced in frequency, then A_j will have several separate peaks, each corresponding to one of the signals. Even if the signals are monochromatic, each peak will contain several of the components A_j, since Δf is greater than zero.

We shall denote the largest component in the peak corresponding to the signal under study as A_i. We take the amplitude of the signal to be measured by the total power in a band centered on A_i, given by

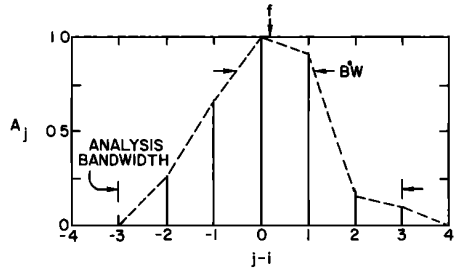

$$P \triangleq \sum_{j=i-3}^{i+3} A_j^2$$

$$f \triangleq \Delta f \; \frac{\sum_{j=i-3}^{i+3} jA_j^2}{P}$$

$$BW \triangleq 2 \left[\frac{\sum_{j=i-3}^{i+3} (j\Delta f - f)^2 A_j^2}{P} \right]^{1/2}$$

Fig. 1. Method of measuring the amplitude, frequency, and bandwidth of a signal. A_i is the largest component in the spectrum. The analysis bandwidth is the frequency range over which the summations are calculated.

$$P \triangleq \sum_{j=i-3}^{i+3} A_j^2 \tag{2}$$

Thus when $\Delta f = 25$ Hz (as is the case for the data in this paper), the amplitude of a signal is found by measuring the total power in a 175-Hz band centered on the signal. This band may seem unnecessarily wide for nearly monochromatic signals but is required to accommodate better the emissions with rapidly changing frequencies.

The frequency of the signal, defined as the average frequency over the band in which the power is measured, is given by

$$f = \left(\Delta f \sum_{j=i-3}^{i+3} jA_j^2 \right) \Big/ P \tag{3}$$

Tests with mathematical test signals [*Stiles*, 1974*b*] show that the frequency given by this equation is practically equivalent to the average frequency of the signal over the period included in the Fourier transform.

The measured bandwidth of the signal, defined as being twice the rms deviation from the frequency defined in (3), is given by

$$BW \triangleq 2 \left[\left(\sum_{j=i-3}^{i+3} (j\Delta f - f)^2 A_j^2 \right) \Big/ P \right]^{1/2} \tag{4}$$

These definitions are summarized in Figure 1.

Under ideal conditions (i.e., mathematical test signals in the absence of noise) these definitions give values that are close to the true values. Because of the linearity of the Fourier transform there is no difficulty in measuring the relative amplitude (P) of different signals (or the change with time of the amplitude of one signal), provided that the signals are sufficiently separated in frequency. P is somewhat sensitive to changes in the f-t slope of a signal. As the slope increases, more of the signal appears outside the bandwidth of the summation, resulting in a decrease in the measured power. For the analysis parameters used in this work ($\Delta t = 40$ ms, $\Delta f = 25$ Hz) the error in the measured amplitude is <1 dB for slopes below 5 kHz/s and increases to ~3 dB at 20 kHz/s.

For monochromatic test tones the measured frequency as defined by (3) differs from the true frequency by much less than 1 Hz over our range of frequencies. For linearly rising tones the maximum error increases with slope, reaching ~1 Hz at 5 kHz/s and 6 Hz at 10 kHz/s.

The bandwidth defined by (4) will vary slightly with the exact frequency of the signal. BW is a minimum whenever the frequency of the signal is equal to a multiple of Δf; it is a maximum midway between two such multiples. The values of the maxima and minima also depend slightly upon the location of the signal in the passband of the Fourier analysis. At the low end of the passband, BW ranges from 26 to 27 Hz, while at the high end the range is 25–26.5 Hz. Most of our signals are located near the center of the passband, where the minimum measurable bandwidth is about 25.5 Hz. In practical applications this variation is considerably smaller than the spread in the data; it is also much less than that obtained when the half-power points of the spectrum are used as a measure of the bandwidth.

The bandwidth is also a function of the slope of the signal. The minimum value of BW increases to ~70 Hz at 5 kHz/s and to 90 Hz at 20 kHz/s. This dependence presents no problems in the analysis of emission characteristics, since the measured bandwidth of the ASE's can be compared to the bandwidth of a test tone of identical slope.

In order to judge the practical usefulness of these definitions, tests have also been carried out on ideal signals that have been corrupted by the addition of noise. The total measured power is simply the sum of the signal power and the noise power in the 175-Hz band over which the summation of (2) is made. In most of the cases covered below, the noise level is more than 10 dB below the signal and represents an error of less than 1 dB. The effect of this level of noise upon the measurement of the frequency is also relatively minor; the error should be less than 1 Hz for ratios of signal-plus-noise to noise greater than 10 dB. This error is generally smaller than the variations within the data and the fluctuations introduced by the instrumentation.

The presence of noise broadens the measured bandwidth by an amount that depends upon the relative amplitudes of the signal and the noise. The measured bandwidth of white noise alone is about 75 Hz. As the signal-to-noise ratio increases, the bandwidth decreases toward its minimum value. For a signal 10 dB above the noise the bandwidth is ~38 Hz; it drops below 30 Hz for signals that are more than 20 dB above the noise.

Aside from noise the principal source of error in the above measurements is the instrumentation used for recording and analyzing the VLF data. The largest error is caused by variations in the speed of the tape recorders. Fortunately, this error is easily corrected by checking accurate timing signals that are recorded simultaneously with the data.

Another source of error was discovered when the definition of frequency given by (3) was first applied to some of the transformed data. The band-pass translator [*Stiles and Helliwell*, 1975], a device that filters out the desired signal and moves it down into the range of the A-D converter, introduces a small amount of frequency modulation. The maximum deviation of this modulation varies from approximately ±4 to ±8 Hz, and its period ranges from 0.1 to 1 s. The modulation may be very regular. In many cases this fluctuation is negligibly small. Where it does become important, it may be compensated for, as is the tape speed error, by referring to a monochromatic signal of known frequency that is also present in the passband (harmonics of 60 Hz are usually available). The variation of the monochromatic signal is measured, and the correction is then made to the signal under study.

When the necessary corrections have been made, the determination of the frequency of a signal by means of (3) may be quite precise. The frequency of a 3.5-kHz whistler mode signal transmitted from Siple Station, Antarctica, and received at Roberval, Quebec, Canada, was found to be ~3.5005 kHz ± 2 Hz from measurements taken over a period of several seconds. The reader may object that we are quoting uncertainties in frequency much less than $1/\Delta t$ = 1/40 ms = 25 Hz. In the present case and in other cases in which we wish to emphasize the precision of the frequency measurements the quoted frequency is actually the average of many measurements. The uncertainty in time is thus increased by a factor equal at least to the number of independent measurements, and the minimum uncertainty in frequency is correspondingly reduced.

3. Results

The first example (Figure 2) shows the signal and emissions received at Roberval, Quebec, that were excited by a 1-s pulse from Siple Station, Antarctica. In Figure 2*a* the display is identical to that of *Stiles and Helliwell* [1975]. Each trace represents the output of one Fourier transformation of 40 ms of data. The frequency range from 5.0 to 6.0 kHz is displayed vertically, and the amplitude of each spectral component is shown increasing to the right. Since adjacent transforms overlap by 50%, the traces are spaced by 20 ms. Sferics cause some interference, notably at −0.08, −0.02, 0.22, and 1.0 s.

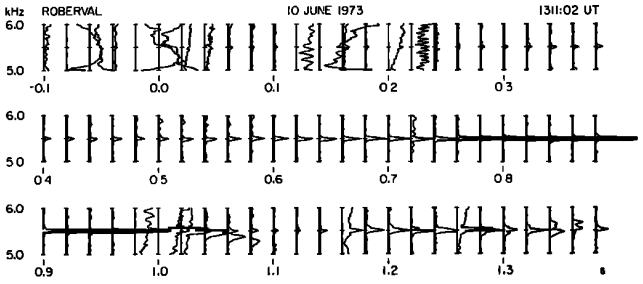

Fig. 2*a*. Spectra of an emission triggered by a 1-s pulse from Siple at 1211:02 UT on June 10, 1973.

In all of the events to be presented in this paper, time is measured from the point when the leading edge of the whistler mode component of the transmitted pulse should arrive at the receiver. In contrast to most of the data presented by *Stiles and Helliwell* [1975] the subionospheric signal from Siple Station is not detectable at the receiver and does not interfere with observations of the relatively weak leading edge of the whistler mode signal. This feature and accurate timing simplify determination of the pulse travel time.

The frequency, amplitude, and bandwidth of the emission of Figure 2*a* are determined by the formulas given in section 2 and are shown in Figure 2*b*. (The solid line in the amplitude plot is a measure of the power in a 175-Hz band that is close to, but does not contain, the signal. This measurement is useful in judging whether variations in the other quantities might be caused by wide band interference, such as sferics.) Before about 0.3 s the frequency (top panel) and amplitude (middle panel) vary widely; the bandwidth (bottom panel) starts at a high value and slowly decreases. This behavior is attributed both to the low initial amplitude of the signal and to the presence of several sferics.

This event is a particularly good example of exponential growth at the transmitter frequency. The amplitude, measured in decibels, shows very little departure from linearity from 0.26 to 0.88 s. (The small bumps near 0.3 and 0.5 s are probably caused by the higher background level at those times.) Thus

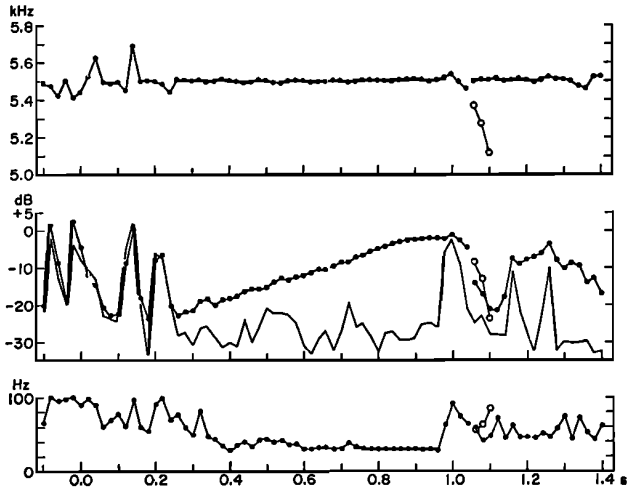

Fig. 2*b*. Frequency, amplitude, and bandwidth of the emission in Figure 2*a*. Open circles are used in this figure and Figure 4*b* when a second significant peak appears in a trace.

growth is purely exponential in time; the measured growth rate for this emission is 33 dB/s. Other emissions in this 5-min run show growth rates that vary from about 27 to 80 dB/s.

The initial portion of the pulse in Figure 2*b* is obscured by several sferics; an examination of less noisy adjacent pulses shows that the initial amplitude of the whistler mode signal is about −24 dB. This value corresponds roughly to those lower points between 0.0 and 0.3 s that are above the noise; these are also the times of lowest bandwidth. We conclude that these points are indeed primarily the signal. Since the leading edge of the pulse shows the same time of arrival as the whistlers on the record, we deduce that the segment from 0.0 to 0.2 s is the unamplified whistler mode signal from the transmitter. Thus growth is first observed about 0.26 s after the onset of the triggering signal. The total growth, up to the point where the amplitude saturates at 0.9 s, is then about 22 dB, or a factor of 158 in power.

We should point out that these last values of time to saturation and total gain are not characteristic of all the events within the run. Some pulses trigger little or no growth. At times the growth may not appear until the last 200 ms or so, possibly because of suppression by another whistler mode signal. In this sequence, growth rarely begins before 0.2 s, but when significant growth does occur, the total gain is about 20–30 dB.

On other days (see the discussion below and the Siple emissions of *Stiles* [1974*b*] and *Stiles and Helliwell* [1975]) the measured growth rates extend up to 250 dB/s. The range of observed growth rates for the triggering signal thus spans 1 order of magnitude from ~25 to ~250 dB/s. Provided the triggering pulse is long enough, the growth usually saturates, as is shown in Figure 2*b* [see also *Stiles and Helliwell*, 1975]. The total growth to saturation is typically in the range of 20–35 dB.

Returning to Figure 2*b*, we see that the measured frequency of the amplified signal remains extremely close to the transmitter frequency of 5.5 kHz. The major deviation from 5.5 kHz (prior to the termination of the triggering pulse at 1.0 s) is caused by the FM introduced by the band-pass translator. If an average is performed over five cycles of this modulation, from 0.4 to 0.9 s, the frequency is found to be 5500.76 Hz. This value is within the experimental error (±1 Hz, due to recording speed uncertainty) of the actual frequency of the transmitted signal.

This event is also an excellent example of the very narrow bandwidth that may be observed. From 0.78 to 0.98 s the measured bandwidth (Figure 2*b*) lies between 27.6 and 30 Hz. The absolute minimum for a monochromatic tone with no interference is about 25.5 Hz at this frequency. For a pure tone which is 20–25 dB above random noise, as is the one in the example, the measured bandwidth is 27.5 Hz. An additional test has been performed in which the signal from an oscillator was combined with noise at −20 dB and then recorded on tape, as is done with the actual data. The measured bandwidth of this signal was about 28.9 Hz. These values and comparisons with the measured bandwidths of rising tones (whose 'true' bandwidth can be calculated from a time domain analog of (4)) suggest that the bandwidth of the amplified signal is no greater than ~10 Hz.

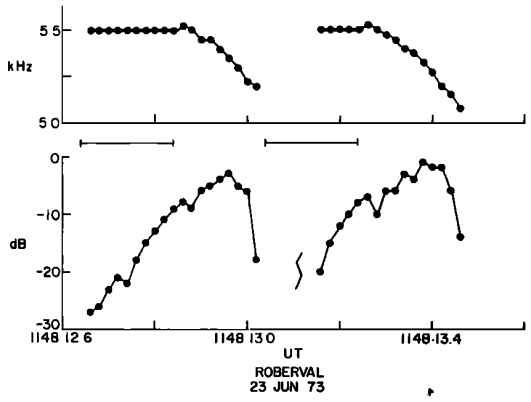

Fig. 3. Frequency and amplitude of emissions triggered by two 200-ms Siple pulses at 1148:12.6 UT on June 23, 1973. The horizontal bars denote the duration of the triggering signals [from *Stiles*, 1974*a*].

The termination of the injected signal and the initial development of the falling emission (visible from 1.02 to 1.1 s) are unfortunately obscured by a sferic. Following the faller, another signal component can be seen to be growing irregularly, with a minimum amplitude at about 1.1 s. This irregularity is probably caused by interference between two signals on different paths. Measurements of whistler delays from Siple recordings taken nearby in time show at least three active paths within the appropriate range of time delays. Since we are concerned primarily with the first component of the signal and its associated emission, we will not consider further these later components.

Additional characteristics of the growth phase of the triggering signal and associated emissions are exhibited by the events shown in Figure 3. (These data, originally appearing in the report by *Stiles* [1974*b*], were analyzed with an earlier processing scheme and thus are presented in a different format. The frequency is shown in units of 25 Hz, the fundamental frequency of the Fourier transform. The amplitude is that of the strongest component and is shown in steps of 1 dB.) The horizontal bars between the upper and the lower panels denote the duration of the 200-ms input signal. The sequence from which these pulses are taken is described in detail by *Stiles and Helliwell* [1975], and these pulses also appear in Figure 5 as the fourth and fifth pulses in the 200-ms set of the 1148:08 UT run.

Of particular interest here are the facts that growth continues after the triggering signal has terminated and that the frequency changes significantly during posttermination growth. Both emissions grow at least 5 dB after termination of the input signal. At the same time the frequency (which is held at the transmitter frequency of 5.5 kHz until termination) first rises about 25 Hz and then falls 200 Hz or more before growth ceases.

Such behavior is common for triggering pulses of intermediate length in this particular run. For shorter input pulses (<150 ms) there was generally no growth of the emission. Since the growth typically saturated at about 260 ms, the longer pulses (≥300 ms) also showed no emission growth following termination. The amplitude reached by the emissions of Figure 3 is within 1 dB of the saturation amplitude of the longer pulse immediately following.

Whereas some transmitter pulses may trigger only single emissions, such as those shown in Figures 2 and 3, others may trigger more than one emission, such as those illustrated in Figure 4. The triggering signal in this case was a 1-s pulse from Siple Station. A rising emission was triggered at 0.2 s, and several additional emissions of rather complex form were triggered near 1.0 s. The process of signal growth, development of the first riser, suppression, and regrowth is well illustrated in Figure 4*b*. The two portions from 0.0 to 0.4 s

and 0.5 to 0.9 s show essentially the same behavior. The pulse starts in the noise at −32 dB and grows to a saturation level of −7 dB with a growth rate of about 110 dB/s, over 3 times the growth rate shown in Figure 2. The measured bandwidth starts high (as is expected for a low signal-to-noise ratio) and drops rapidly as the amplitude increases. About 300 ms after the start of growth the bandwidth increases and varies more widely. The increase in the bandwidth coincides with the onset of the emission.

The principal difference between the two portions is in the nature of the emissions. The first is a well-developed riser. The second is several decibels weaker and turns into an inverted hook (rises and then falls). This behavior is typical of the run. The second emission is rarely as strong and well defined as the first, unless it occurs very near the end of the triggering pulse. It appears that the first riser suppresses the oscillation at the transmitter frequency, forcing the growth process to start over. The transmitter signal reemerges from the noise just before 0.5 s, about 0.2 s after the first riser begins, and it reaches the same level that it reached before.

The behavior of the second emission is complex. At 1.06 s it either collides with or crosses a riser that originated at 0.96 s. This interaction yields a second inverted hook (the dip in frequency at 0.96 s being neglected) and a normal hook. The two emissions approach one another near 1.32 s, and the normal hook finishes with a smooth rise in frequency.

The second inverted hook is very clean. At its apex the measured bandwidth drops to 30 Hz, which is close to the measured bandwidth of a monochromatic signal. Similar bandwidths have been measured on other off-frequency emissions, indicating that the bandwidth can approach the minimum measurable, even in the absence of a triggering signal.

Multiple triggering has also been observed in many of the Omega data [e.g., *Stiles and Helliwell,* 1975]. The evidence suggests that these multiple emissions are usually triggered on the same path. When the leading edge of the triggering pulse and its termination (as often shown by a jump in bandwidth and the appearance of off-frequency components) are detectable, as is frequently the case, their time difference equals the transmitted pulse length, thus supporting the conclusion that triggering is occurring along a single whistler mode path. In all cases of multiple triggering by a constant signal, falling tones are generally not observed until after the signal has ended.

Our last example (Figure 5) is a sequence of several minutes of data from Siple transmissions on 5.5 kHz, two pulses from which are shown in Figure 4. (A portion of this run was discussed by *Helliwell and Katsufrakis* [1974] and *Stiles and Helliwell* [1975].) Each 18-s segment of this sequence consists of eight sets of five pulses each, in which the pulse length increases in increments of 50 ms, from 50 ms to 400 ms. The spacing between pulses equals their lengths.

Just prior to the data shown in Figure 5 there was little emission activity. Then fallers began to appear, their intensity increasing with pulse length, as is shown in the top panel. As the emissions became stronger, more rising tones were triggered by the longer pulses, and falling tones were triggered by the shorter pulses. Following the peak in activity (roughly 1147:50 UT) the emissions became weaker, and fewer risers were seen. As the activity died out, the risers disappeared altogether, and only fallers remained, being triggered only by pulses of 300-ms or greater duration. Measurements of the growth rates during this run show that higher rates coincided with the stronger emissions (and risers), while lower growth rates were associated with the beginning and ending of the

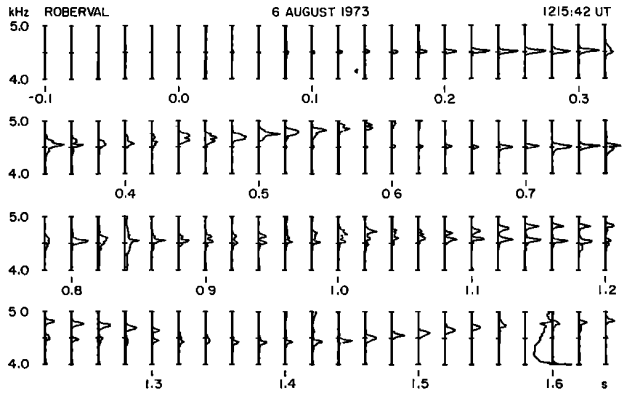

Fig. 4*a*. Spectra of an emission triggered by a 1-s pulse from Siple at 1215:42 UT on August 6, 1973. The pulse begins at 0.0 s.

sequence. (A similar sequence of weaker signals and emissions was seen at a lower transmitter frequency and slightly earlier in time.)

The sequence described above (fallers, risers, and fallers) is quite common. Activity at NAA and Siple often begins with falling tones. As the emissions become stronger, risers appear. When activity fades, the risers disappear. Fallers are often the last emissions seen prior to the cessation of activity. Several such cases have been documented by *Stiles* [1974*b*].

4. Discussion

As an aid to discussion we summarize below the principal triggering phenomena that we have observed inside the plasmapause. These statements apply to Siple Station fixed-frequency transmissions on ducted paths near $L = 4$ and at frequencies in the vicinity of 5 kHz.

1. Signals may grow exponentially with time at rates ranging from 25 to 250 dB/s, the frequency of the output signal being equal to that of the input signal.
2. Growth may cease when the input signal terminates, or it may continue for several decibels during the course of an emission.
3. Maximum temporal growth is 20–35 dB for either the signal or the emission.
4. Both the amplified signal and the triggered emissions

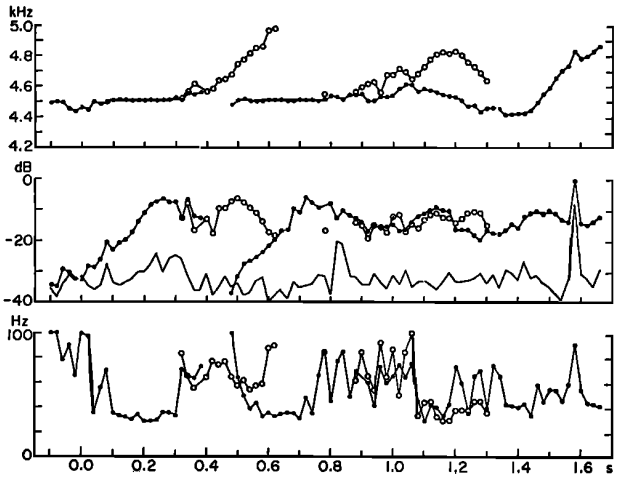

Fig. 4*b*. Frequency, amplitude, and bandwidth of the emission in Figure 4*a*.

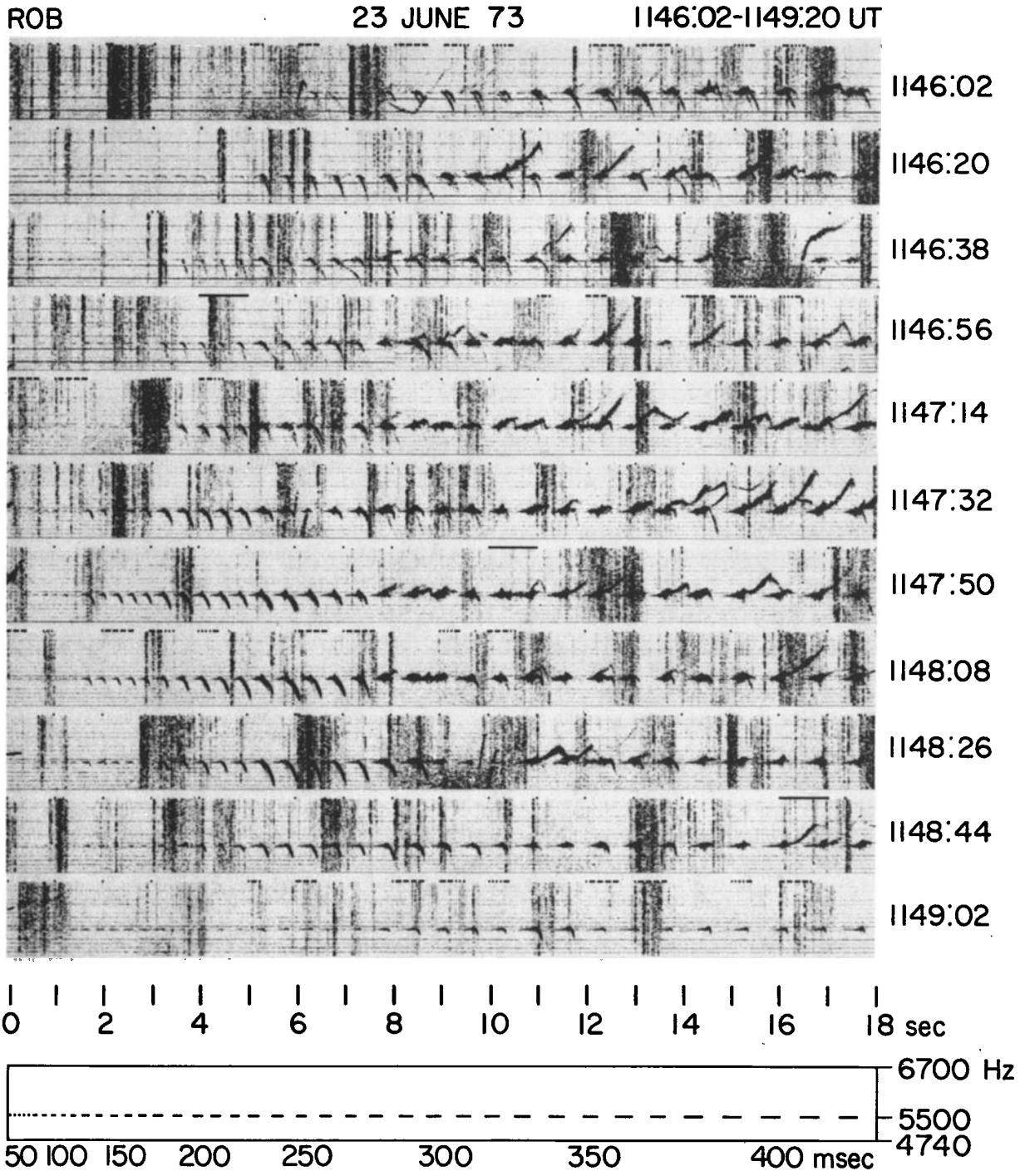

Fig. 5. Compressed spectra from June 23, 1973, showing how the transition from fallers to risers moves to shorter pulse lengths as growth rates increase. (The ninety-first harmonic of the power system appears 40 Hz below the transmitter frequency.)

may exhibit maximum measurable coherence (i.e., minimum resolvable bandwidth).

5. The growth and decay of an emission are essentially independent of its frequency variation.

These results are consistent with those of other experiments. Recently, *McPherson et al.* [1974] analyzed signals triggered by a VLF transmitter in Alaska and received in New Zealand. They found that the amplitude increased with increasing pulse length up to 0.25 s and then leveled off (with perhaps a slight decrease as the length increased further). This behavior is in accord with our observation of exponential growth up to a saturation level.

A similar experiment using station NSS on 15.5 kHz was performed in 1959 [*Helliwell*, 1965]. Pulses of 600-ms length produced strong whistler mode signals, but 100-ms pulses produced no detectable output. These results are now readily explained in terms of the exponential growth rates measured in the present experiment. A good example is seen in the top

panel of Figure 5, where the 100-ms pulses are at the threshold of detection, while the 400-ms pulses have reached saturation.

The growth rates of natural emissions outside the plasmapause are discussed by *Burtis and Helliwell* [1975]. These emissions, which are apparently spontaneous (i.e., not triggered by another signal), show exponential growth rates ranging from about 200 to 2000 dB/s. In contrast, the signal growth of the present experiment shows rates ranging from 25 to 250 dB/s. These results are not necessarily inconsistent. As *Burtis and Helliwell* [1975] point out, a much higher growth rate should be required to produce a narrow band emission when the input is broad band noise than when it is a monochromatic transmitter pulse.

In a recent study, *Helliwell and Crystal* [1973] used an idealized computer simulation model of the emission generation process to predict the amplitude behavior. They assumed a monoenergetic stream of electrons in a homogeneous interaction region of limited length, centered on the geomagnetic equator. The transmitter signal enters the region from one direction, causing phase bunching of resonant electrons entering from the opposite direction. The resulting radiation from the bunched electrons bunches more electrons, thus establishing a feedback loop which generates the emission. When the exciting signal is turned off, exponential growth continues up to a saturation level set by the parameters of the model. The present experiment shows similar behavior, illustrated in Figure 3.

It should be recalled, however, that not all of the ASE's continue to grow past termination of the input signal. Very few of the emissions triggered by the shorter (<200 ms) pulses of June 23, 1973, exhibited growth. The amplitude must apparently reach a certain level before the growth can become self-sustaining. This result does not appear in the model. However, neither noise nor interfering signals were included in the model, and hence there was no other signal that could interfere with growth at the triggering frequency.

The observation that emission growth tends to be independent of frequency change, as shown in Figure 3, is in accord with the prediction of *Helliwell* [1970]. There it was shown that the interaction length is relatively insensitive to df/dt and hence the growth rate should not depend on df/dt.

One of the goals of this work has been to ascertain the factors determining the final slope of the emissions. It has long been known [*Lasch*, 1969] that increasing the length of the transmitted pulse may change the final slope of the emissions from negative to positive. There are many instances, however, where a pulse of one length may trigger both risers and fallers (Figure 5). The present study indicates that for a given pulse length the final slope of the emission may also be related to the growth rate of the input signal. For example, compare the signal of Figure 2 to that of Figure 5; see also the sequence of Figure 5, where higher growth rates were measured in the groups that produced risers. An examination of these data and emissions triggered by NAA pulses suggests that risers will be produced by sufficiently long pulses when the growth rate is high enough ($\gtrsim$100 dB/s); fallers will be produced by short pulses and/or low growth rates ($\lesssim$50 dB/s).

The results of *Helliwell and Crystal* [1973] for a monochromatic stream may help explain the relation of the growth rate to the final slope. There it was found that the triggering of self-sustaining emissions will only occur if the flux of resonant electrons exceeds a certain value; furthermore, the growth rate is roughly proportional to the flux above the minimum. We shall also refer to *Helliwell*'s [1967] result for the time rate of change of the frequency of an emission as a function of the location of the generation region ($df/dt = Ks$, where s is the distance from the equator in the direction of streamflow and K is a constant that depends on the inhomogeneity of the medium and on the refractive index). The slope is zero at the equator, positive on the downstream (transmitter) side, and negative on the upstream (receiver) side.

On the basis of these ideas it can be argued that the growth rate should maximize at the equator. As the emission generation region moves off the equator, the flux of resonant electrons (and thus the growth rate) will decrease. The reason is that the wave frequency must be Doppler-shifted up to the local gyrofrequency by the electrons' parallel velocity and the resonant electrons must therefore have a higher parallel velocity. Since the flux of electrons generally falls off rapidly with increasing velocity [*Frank*, 1966], fewer particles are available for the interaction; this argument was first advanced by *Brice* [1964*a*]. In addition, the length of the interaction region is reduced, a constant frequency being assumed, causing a loss of output for a given flux [*Helliwell*, 1970].

Thus the growth rate for a constant frequency triggering signal should maximize on the equator. If the flux exceeds the minimum required at the equator, then it should be sufficient some distance downstream to produce risers. (Note that the triggering signal always encounters the riser region first.) On the other hand, if the equatorial flux is barely sufficient to sustain emissions, we will expect ASE's to be triggered only near the equator. Their frequency slopes would then be small, and the interaction region would tend to drift across the equator in the direction of wave propagation, the result being that falling tones would occur. Thus lower growth rates should be associated with nearly constant frequency or falling tones. In this way we account for the characteristic sequence of fallers, risers, and fallers associated with the buildup and decay of growth and emission activity.

An important feature of triggered emissions is the gain in wave energy that results from the interaction. Usually, much more energy is released than is injected into the interaction region. The energy output will control the amount of pitch angle scattering of the interacting electrons. Hence it could be a convenient index of particle precipitation. We define the energy gain as $G_E = W_o/W_i$, where W_o is the total output wave energy, including both temporal growth of the triggering signal and any emissions; and W_i is the signal input energy.

Assume that there is no spectral broadening and that the emissions and the triggering signal travel on the same path. Then we obtain W_i by squaring the amplitude at the leading edge of the triggering signal and multiplying by the pulse length. W_o is obtained by integrating the squared output amplitude over the duration of signal plus associated emissions. Applying this procedure to the first path of Figure 2, we obtain $G_E \simeq 54$. The corresponding peak power output is 158 times the input power. For long-enduring ASE's, on the other hand, the value of G_E can exceed the power gain. For example, if we assume that the risers triggered by 400-ms pulses in Figure 5 are 1 s long and 30 dB above the input signal, the peak power gain is 1000, while the energy gain is over 2000. Energy gain could be employed in studies aimed at finding the optimum transmitter parameters for maximizing the precipitated flux.

Acknowledgments. We acknowledge discussions with our colleagues in the Radioscience Laboratory at Stanford University. Particularly helpful comments were made by D. L. Carpenter, C. G. Park, and T. L. Crystal. The research was supported in part by the Office of Polar Programs, National Science Foundation, under

grant GV-28840X; in part by the Atmospheric Sciences Section, National Science Foundation, under grant GA-32590X; and in part by the U.S. Air Force Office of Scientific Research under grant F44620-72-C-0058. Completion of this work by G.S.S. was made possible by support from the Los Alamos Scientific Laboratory and the Energy Research and Development Administration.

The Editor thanks R. L. Dowden and H. C. Koons for their assistance in evaluating this paper.

REFERENCES

Bell, T. F., ULF wave generation through particle precipitation induced by VLF transmitters, *J. Geophys. Res., 81,* 3316, 1976.

Bergland, G. O., A guided tour of the fast Fourier transform, *IEEE Spectrum, 6,* 41, 1969.

Brice, N. M., Discrete VLF emissions from the upper atmosphere, *Tech. Rep. 3412-6,* Stanford Electron. Lab., Stanford Univ., Stanford, Calif., 1964*a*.

Brice, N. M., Fundamentals of VLF emission generation mechanisms, *J. Geophys. Res., 69,* 4515, 1964*b*.

Burtis, W. J., and R. A. Helliwell, Magnetospheric chorus: Amplitude and growth rate, *J. Geophys. Res., 80,* 3265, 1975.

Carpenter, D. L., and C. G. Park, On what ionospheric workers should know about the plasmapause-plasmasphere, *Rev. Geophys. Space Phys., 11,* 133, 1973.

Frank, L. A., Several observations of low-energy protons and electrons in the earth's magnetosphere with Ogo 3, *Rep. 66-48,* Dep. of Phys. and Astron., Univ. of Iowa, Iowa City, 1966.

Helliwell, R. A., *Whistlers and Related Ionospheric Phenomena,* Stanford University Press, Palo Alto, Calif., 1965.

Helliwell, R. A., A theory of discrete VLF emissions, in *Particles and Fields in the Magnetosphere,* edited by B. M. McCormac, pp. 292–301, D. Reidel, Dordrecht, Netherlands, 1970.

Helliwell, R. A., and T. L. Crystal, A feedback model of cyclotron interaction between whistler mode waves and energetic electrons in the magnetosphere, *J. Geophys. Res., 78,* 7357, 1973.

Helliwell, R. A., and J. P. Katsufrakis, VLF wave injection into the magnetosphere from Siple Station, Antarctica, *J. Geophys. Res., 79,* 2511, 1974.

Helliwell, R. A., J. P. Katsufrakis, and M. L. Trimpi, Whistler-induced amplitude perturbation in VLF propagation, *J. Geophys. Res., 78,* 4679, 1973.

Helliwell, R. A., J. P. Katsufrakis, T. F. Bell, and R. Raghuram, VLF line radiation in the earth's magnetosphere and its association with power line radiation, *J. Geophys. Res., 80,* 4249, 1975.

Lasch, S., Unique features of VLF noise triggered in the magnetosphere by Morse code dots from NAA, *J. Geophys. Res., 74,* 1856, 1969.

McPherson, D. A., H. C. Koons, M. H. Dazey, R. L. Dowden, L. E. S. Amon, and N. R. Thompson, Conjugate magnetospheric transmissions at VLF from Alaska to New Zealand, *J. Geophys. Res., 79,* 1555, 1974.

Otnes, R. K., and L. Enochson, *Digital Time Series Analysis,* John Wiley, New York, 1972.

Rosenberg, T. J., R. A. Helliwell, and J. P. Katsufrakis, Electron precipitation associated with discrete very low frequency emission, *J. Geophys. Res., 76,* 8445, 1971.

Stiles, G. S., Controlled VLF experiments, in *ELF-VLF Radio Wave Propagation,* edited by J. Holtet, D. Reidel, Dordrecht, Netherlands, 1974*a*.

Stiles, G. S., Digital spectra of artificially stimulated VLF emissions, *Tech. Rep. 3465-3,* Radiosci. Lab., Stanford Electron. Lab., Stanford Univ., Stanford, Calif., 1974*b*.

Stiles, G. S., and R. A. Helliwell, Frequency-time behavior of artificially stimulated VLF emissions, *J. Geophys. Res., 80,* 608, 1975.

(Received April 12, 1976;
accepted September 17, 1976.)